

Supporting Information

for

Hole-Rich CoP Nanosheets with Optimized d-band Center for Enhancing pH-Universal Hydrogen Evolution Electrocatalysis

Shuo Geng^{#a}, Fenyang Tian^{#a}, Menggang Li^a, Xin Guo^a, Yongsheng Yu^{a*}, Weiwei Yang^{a*} and Yanglong Hou^{b*}

^aMIIT Key Laboratory of Critical Materials Technology for New Energy Conversion and Storage, School of Chemistry and Chemical Engineering, Harbin Institute of Technology, Harbin, Heilongjiang 150001, China

^bCollege of Engineering, Peking University, Beijing 100871, China

[#] These authors contributed equally.

Corresponding Authors *E-mail: ysyu@hit.edu.cn, yangww@hit.edu.cn and hou@pku.edu.cn

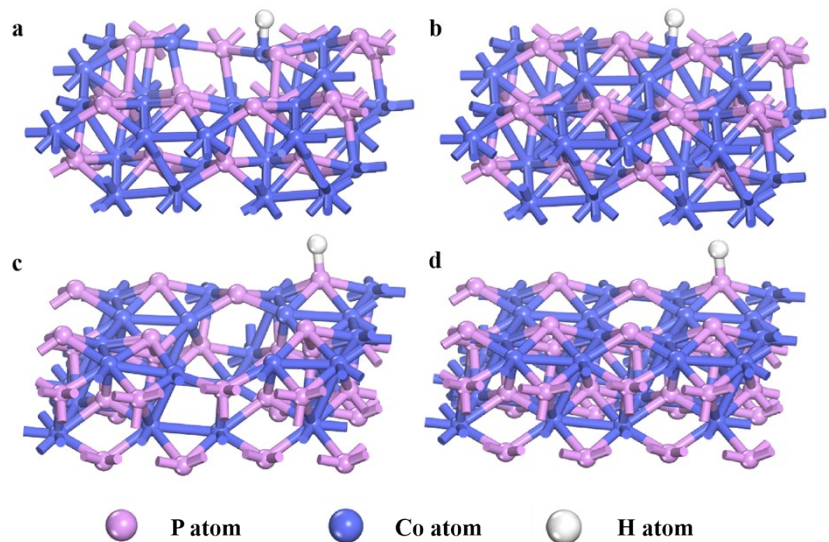


Fig. S1 The models of H adsorption on CoP (a, c) with holes and (b, d) without holes.

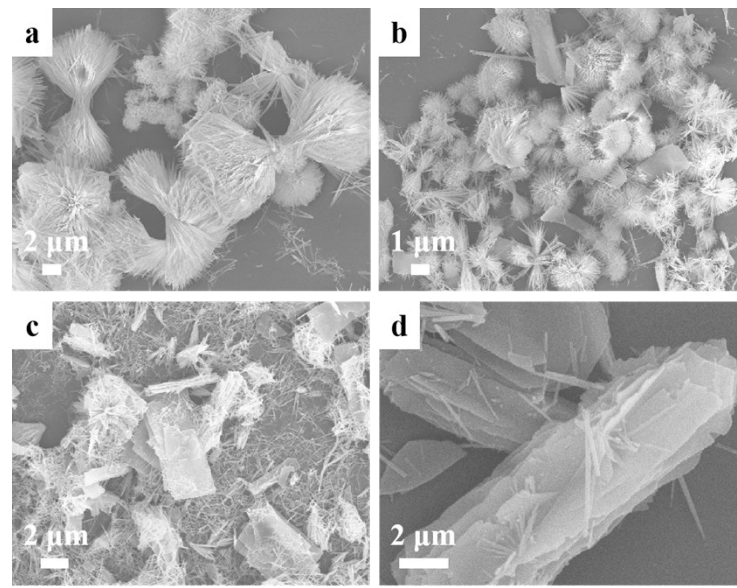


Fig. S2 The SEM images of the precursor at different reaction stages. (a) 2 h, (b) 4 h, (c) 8 h and (d) 11 h.

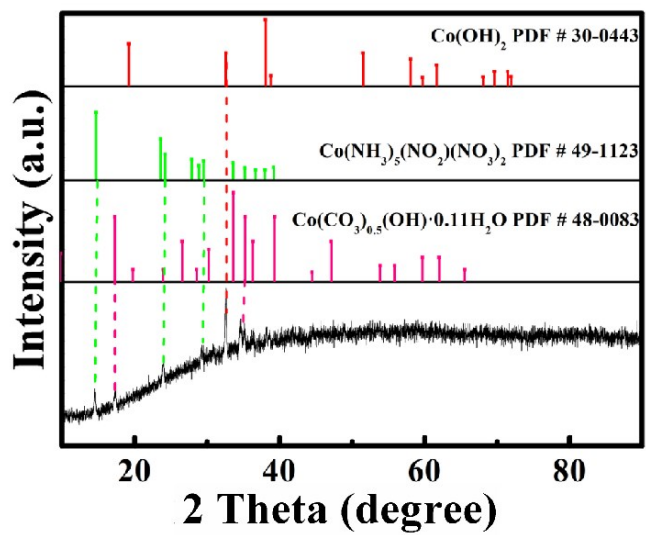


Fig. S3 The XRD pattern of Co-contained precursor.

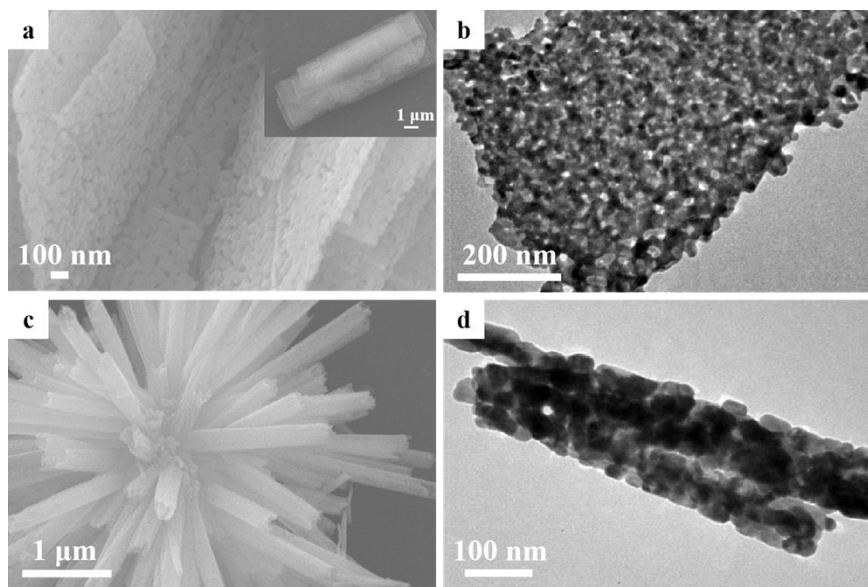


Fig. S4 The SEM images of Co₃O₄ (a) with P123 and without P123 (c). The TEM images of Co₃O₄ with P123 (b) and without P123 (d).

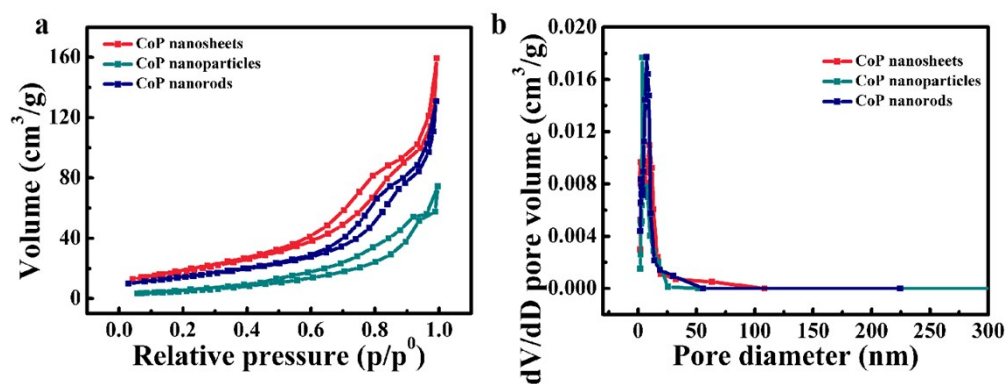


Fig. S5 (a) Nitrogen adsorption/desorption isotherms and (b) BJH pore-size distribution curves of different CoP electrocatalysts.

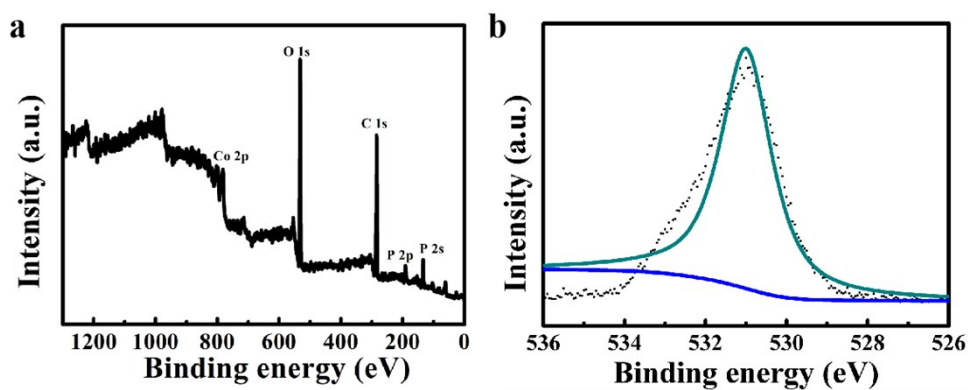


Fig. S6 The XPS survey scan of hole-rich CoP nanosheets (a) and the high resolution XPS spectra of O 1s in CoP nanosheets (b).

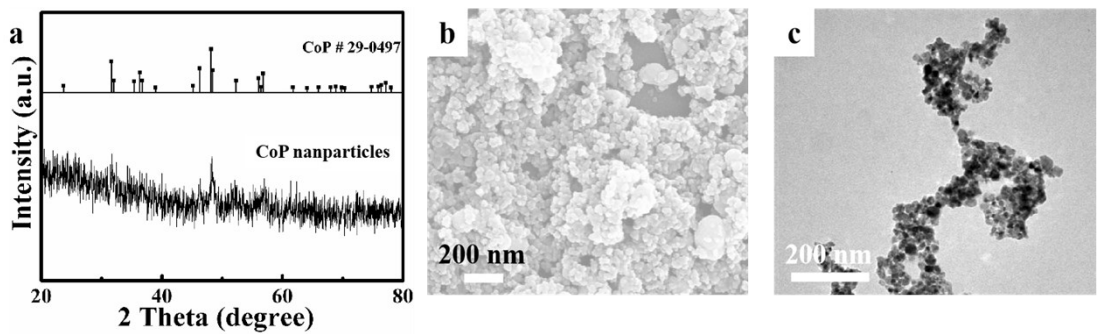


Fig. S7 (a) XRD pattern, (b) SEM image and (c) TEM image of CoP nanoparticles.

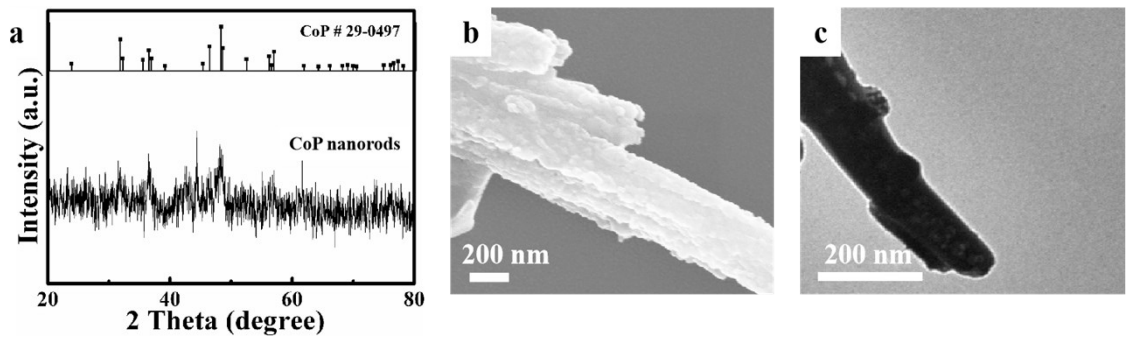


Fig. S8 (a) XRD pattern, (b) SEM image and (c) TEM image of CoP nanorods.

The XRD pattern of the CoP nanoparticles in Figure S7a and CoP nanorods in Figure S8a show the CoP nanoparticles and CoP nanorods have the same spinel phase with CoP nanosheets (PDF no.29-0497). The SEM images (Figure S7b and S8b) and TEM images (Figure S7c and S8c) show that CoP nanoparticles and CoP nanorods have been successfully synthesized, respectively.

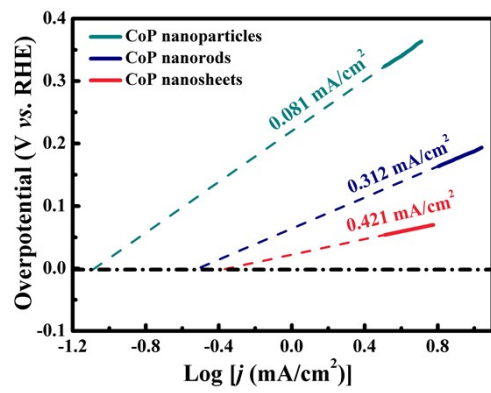


Fig. S9 Calculated exchange current densities of various samples by using extrapolation methods in 0.5 M H_2SO_4 solution.

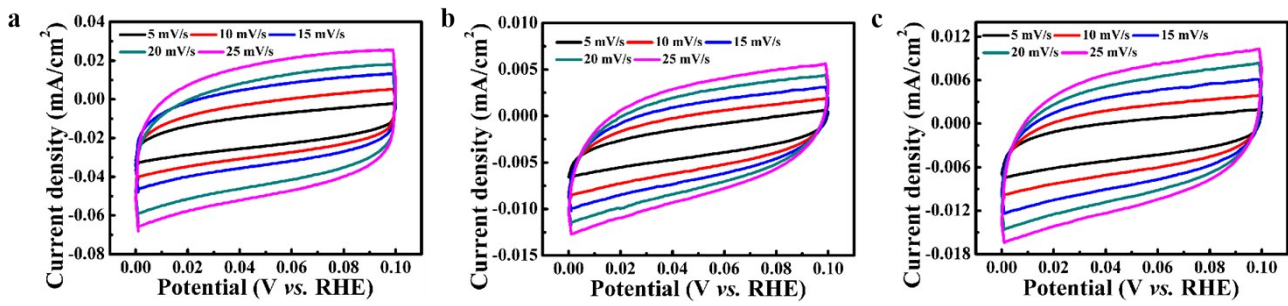


Fig. S10 Cyclic voltammograms (CV) curves of (a) CoP nanosheets, (b) CoP nanoparticles and (c) CoP nanorods in region of 0-0.1 V vs. RHE with various scan rates in 0.5 M H₂SO₄ solution.

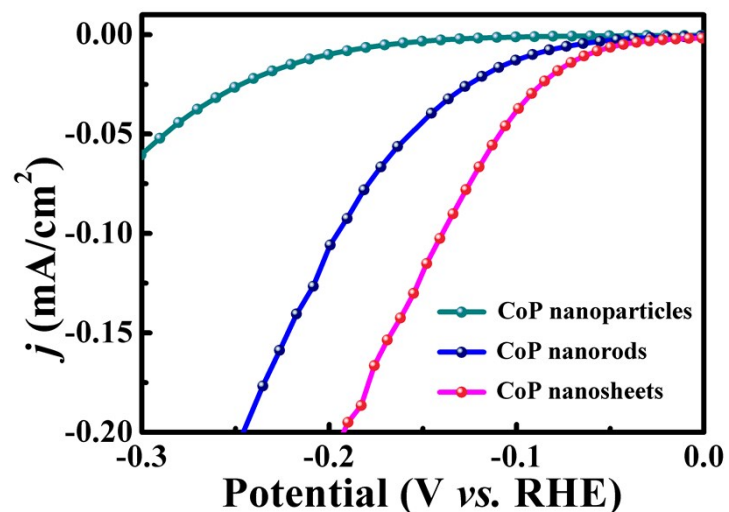


Fig. S11 The HER polarization curves of CoP nanosheets, CoP nanoparticles and CoP nanorods normalized to the ECSA in 0.5 M H₂SO₄ solution.

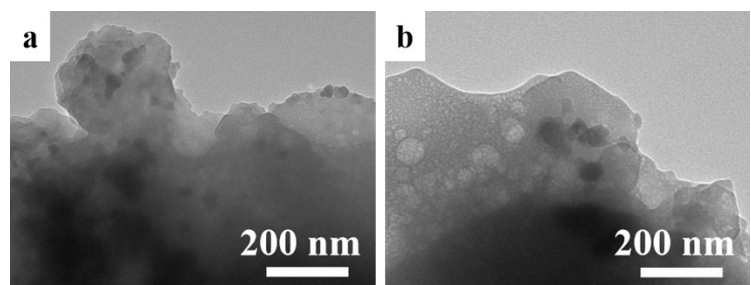


Fig. S12 The TEM images of CoP nanosheets after long-term stability tests in (a) 0.5 M H_2SO_4 and (b) 1.0 M KOH.

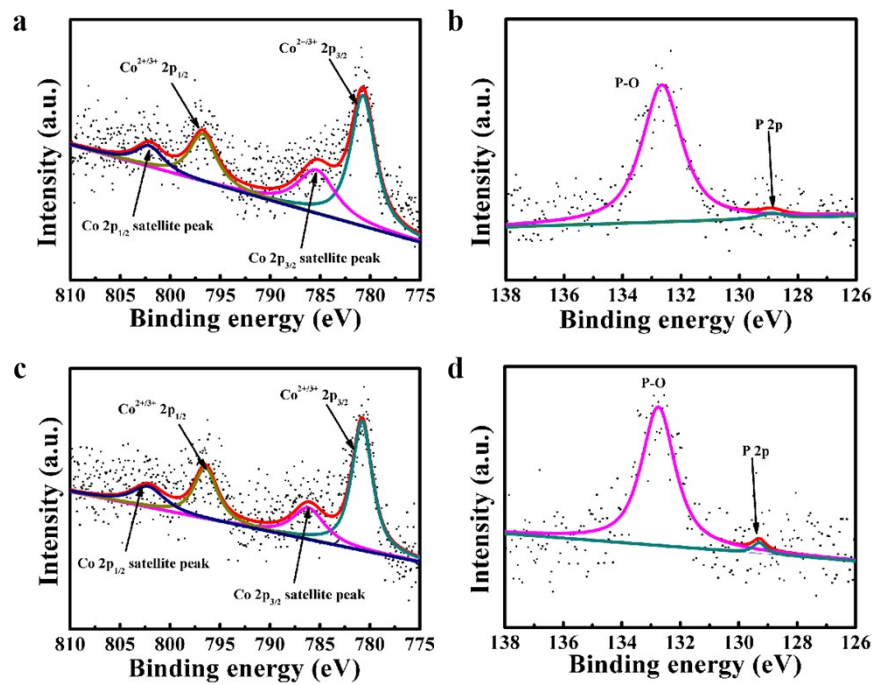


Fig. S13 The high resolution XPS spectra of (a) Co 2p and (b) P 2p of hole-rich CoP nanosheets after long-term stability tests in 0.5 M H_2SO_4 . High resolution XPS spectra of (c) Co 2p and (d) P 2p of hole-rich CoP nanosheets after long-term stability tests in 1.0 M KOH.

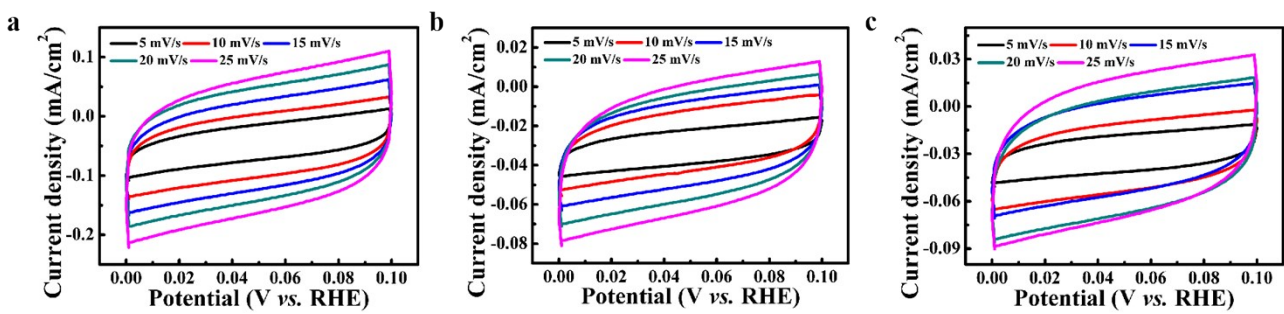


Fig. S14 Cyclic voltammograms (CV) curves of (a) CoP nanosheets, (b) CoP nanoparticles and (c) CoP nanorods in region of 0-0.1 V vs. RHE at various scan rates in 1.0 M KOH solution.

Table S1. Calculated surface energies of hole-rich CoP surfaces.

CoP	(011)	(112)	(211)	(301)
surface energy (meV Å ²)	191.69	222.93	220.04	226.36

Table S2. Comparison the overpotential at a current density of 10 mA/cm² in acidic and alkaline electrolytes.

Catalysts	η_{10} , acid (mV)	η_{10} , alkaline (mV)	References
Hole-rich CoP nanosheets	84	94	This work
CoP	113	154	1
CoP@BCN	87	215	2
CoP@NC/rGO	123.8	NA	3
CoP	160	175	4
CoP/NiCoP	125	133	5
Co(OH) _x @CoP	NA	100	6
Ni-CoP/HPFs	144	92	7
Co ₂ P	95	NA	8
CoP	159	NA	9
CoP@NC	78	129	10
HNDCM-Co/CoP	138	135	11
CoP-NC	NA	154	12
Co ₂ P	NA	160	13
CoP/CNT	122	NA	14
CoP/CoP ₂	NA	138	15

NA: Not available.

REFERENCES

1. H. Li, X. Zhao, H. Liu, S. Chen, X. Yang, C. Lv, H. Zhang, X. She, D. Yang, *Small*, 2018, **14**, 1802824.
2. H. Tabassum, W. Guo, W. Meng, A. Mahmood, R. Zhao, Q. Wang, R. Zou, *Adv. Energy Mater.*, 2017, **7**, 1601671.
3. X. Zhao, D. Luo, Y. Wang, Z. H. Liu, *Nano Res.*, 2019, **12**, 2872-2880.
4. A. Sumboja, T. An, H. Y. Goh, M. Lubke, D. P. Howard, Y. Xu, A. D. Handoko, Y. Zong, Z. Liu, *ACS Appl. Mater. Interfaces*, 2018, **10**, 15673-15680.
5. Y. Lin, K. Sun, S. Liu, X. Chen, Y. Cheng, W. C. Cheong, Z. Chen, L. Zheng, J. Zhang, X. Li, Y. Pan, C. Chen, *Adv. Energy Mater.*, 2019, **9**, 1901213.
6. L. Su, X. Cui, T. He, L. Zeng, H. Tian, Y. Song, K. Qi, B. Y. Xia, *Chem. Sci.*, 2019, **10**, 2019-2024.
7. Y. Pan, K. Sun, Y. Lin, X. Cao, Y. Cheng, S. Liu, L. Zeng, W. C. Cheong, D. Zhao, K. Wu, Z. Liu, Y. Liu, D. Wang, Q. Peng, C. Chen, Y. Li, *Nano Energy*, 2019, **56**, 411-419.
8. J. F. Callejas, C. G. Read, E. J. Popczun, J. M. McEnaney, R. E. Schaak, *Chem. Mater.*, 2015, **27**, 3769-3774.
9. M. Liu, J. Li, *ACS Appl. Mater. Interfaces*, 2016, **8**, 2158-2165.
10. F. Yang, Y. Chen, G. Cheng, S. Chen, W. Luo, *ACS Catal.*, 2017, **7**, 3824-3831.
11. H. Wang, S. Min, Q. Wang, D. Li, G. Casillas, C. Ma, Y. Li, Z. Liu, L. J. Li, J. Yuan, M. Antonietti, T. Wu, *ACS Nano*, 2017, **11**, 4358-4364.

12. B. You, N. Jiang, M. Sheng, S. Gul, J. Yano, Y. Sun, *Chem. Mater.*, 2015, **27**, 7636-7642.
13. K. Xu, H. Ding, M. Zhang, M. Chen, Z. Hao, L. Zhang, C. Wu, Y. Xie, *Adv. Mater.*, 2017, **29**, 1606980.
14. Q. Liu, J. Tian, W. Cui, P. Jiang, N. Cheng, A. M. Asiri, X. Sun, *Angew. Chem. Int. Ed.*, 2014, **53**, 6710-6714.
15. W. Li, S. Zhang, Q. Fan, F. Zhang, S. Xu, *Nanoscale*, 2017, **9**, 5677-5685.